MOLECULAR AND CELLULAR BIOLOGY, Sept. 2003, p. 6174–6186 Vol. 23, No. 17
0270-7306/03/$08.00+0 DOI: 10.1128/MCB.23.17.6174–6186.2003

ZIP Kinase Triggers Apoptosis from Nuclear PML Oncogenic Domains

Taro Kawai,[1] Shizuo Akira,[2] and John C. Reed[1]*

The Burnham Institute, La Jolla, California 92037,[1] and Department of Host Defense, Research Institute for Microbial Diseases, Osaka University, Osaka, Japan[2]

Received 10 March 2003/Returned for modification 15 April 2003/Accepted 14 May 2003

PML oncogenic domains (PODs), also referred to as nuclear dot 10 bodies, Kreb's bodies, or nuclear bodies, represent nuclear structures implicated in the regulation of a variety of cellular processes, including transcription, tumor suppression, and apoptosis. ZIP kinase (ZIPK) is a proapoptotic protein kinase with homology to DAP kinase, a protein kinase implicated in apoptosis. We show here that ZIPK is present in PODs, where it colocalizes with and binds to proapoptotic protein Daxx. Arsenic trioxide (As_2O_3) and gamma interferon (IFN-γ), which accentuate POD formation, increased the association of ZIPK with PODs. In contrast, the kinase-inactive ZIPK resides in nuclei with a diffuse pattern and significantly prevents the association of Daxx with PODs, implying that ZIPK recruits Daxx to PODs via its catalytic activity. ZIPK also binds and phosphorylates proapoptotic protein Par-4. Association of ZIPK with Daxx was enhanced by coexpression of Par-4. Activation of caspases and induction of apoptosis were also observed in cells overexpressing these proteins. Conversely, small-interfering RNA-mediated reduction of ZIPK, Daxx, or Par-4 expression decreased activation of caspase and apoptosis induced by As_2O_3 and IFN-γ. These results suggest that ZIPK, in collaboration with Daxx and Par-4, mediates a novel nuclear pathway for apoptosis.

Programmed cell death is an evolutionarily conserved mechanism for eliminating cells, which plays central roles in embryogenesis and adult tissue homeostasis. In animal species, programmed cell death usually occurs by apoptosis, involving characteristic changes in cell morphology and ultrastructure associated with this route of cell demise. The morphological changes associated with apoptosis can be attributed directly or indirectly to the activation of a family of intracellular cysteine proteases, called caspases (39). Numerous inputs into caspase activation pathways probably exist, only some of which have been delineated in detail. For example, pathways for caspase activation have been linked to (i) mitochondria, which release proteins into the cytosol that facilitate caspase activation; (ii) tumor necrosis factor (TNF)/Fas family cytokine receptors, which recruit caspases to ligand-activated receptor complexes at the cell membrane; and (iii) cytolysis by killer T cells, which inject caspase-activating protease granzyme B into target cells (15, 16, 30, 31, 49).

Protein phosphorylation represents an important mechanism for regulating apoptosis pathways. For example, the protein kinase Akt suppresses apoptosis through its ability to phosphorylate multiple substrates of relevance to apoptosis regulation, including Bcl-2/Bcl-X_L antagonist BAD, human caspase 9, and p53 antagonist Mdm2 (2, 7, 52, 54). Conversely, Ask1, a mitogen-activated protein kinase kinase kinase (MAP3K), reportedly induces apoptosis, possibly through pathways involving Jun N-terminal kinases (19).

ZIP kinase (ZIPK; also known as Dlk) was originally identified as a serine/threonine-specific protein kinase that binds ATF4, a member of the activating transcription factor/cyclic AMP-responsive element binding protein family of transcription factors (23, 25). ZIPK oligomerizes through its C-terminal leucine zipper (LZ) structure, thereby becoming an active enzyme. Ectopic expression of ZIPK in NIH 3T3 cells induces apoptosis. In contrast, the kinase-inactive mutant protein ZIPK (K42A) failed to induce apoptosis, indicating that ZIPK stimulates apoptosis by its catalytic activity (23). The kinase domain of ZIPK shows strong homology to the kinase domain of the death-associated protein kinase (DAPK). Using a functional cloning strategy involving transfection of a gamma interferon (IFN-γ)-sensitive HeLa cell line with retroviral cDNA libraries, Deiss et al. found that cDNA fragments representing DAPK in antisense orientation blocked apoptosis induced by IFN-γ (8). Conversely, overexpression of DAPK induces apoptosis (5). Furthermore, evidence that the gene encoding DAPK may function as a tumor suppressor gene has been presented (20, 38).

ZIPK and DAPK constitute members of a family of related kinases that includes DAPK2 (also known as DRP-1), DRAK1, and DRAK2. These proteins all have strong amino acid sequence homology within their catalytic domains and induce apoptosis upon overexpression (21, 24, 26, 27, 43, 45). Thus, these proteins define a family of protein kinases whose elevated catalytic activity is sufficient for induction of apoptosis. However, the mechanisms responsible for activation of these kinases and the downstream substrates that mediate their apoptotic activity remain unknown.

Apoptosis is initiated from certain organelles, including mitochondria, the endoplasmic reticulum, and possibly the Golgi, in response to specific types of stimuli or stress (6, 13, 39). A nuclear pathway linked to apoptosis has also been suggested by studies implicating PML and the PML-binding protein Daxx in apoptosis sensitization (42). PML and Daxx are nuclear proteins which reside in PML oncogenic domains (PODs), also

* Corresponding author. Mailing address: The Burnham Institute, 10901 North Torrey Pines Rd., La Jolla, CA 92037. Phone: (858) 646-3140. Fax: (858) 646-3194. E-mail: reedoffice@burnham.org.

called nuclear dot 10 bodies, Kreb's bodies, or nuclear domains, which exist in all nucleated mammalian cells. In human acute promyelomonocytic leukemias, the *PML* gene is fused to the retinoic acid receptor α (RARα) gene as a result of t(15; 17) chromosomal translocations, producing PML-RAR chimeric proteins that disrupt PODs and cause an apoptosis-resistant state (9, 22, 42). Disruption of the *pml* gene in mice results in a state of broad apoptosis resistance, including diminished sensitivity to Fas ligand, TNF-α, X-irradiation, ceramide, and IFN-γ (17, 50). Conversely, overexpression of the PML protein induces apoptosis (37). Similarly, overexpression of the PML-binding protein Daxx sensitizes cells to apoptosis induced by TNF family death receptors, while dominant-negative forms of Daxx interfere with apoptosis triggered by the death receptors (48). Taken together, these findings suggest that nuclear PODs participate in a novel pathway for apoptosis.

Here, we report that ZIPK binds and colocalizes in PODs with Daxx. ZIPK localization into PODs requires its catalytic activity, since a kinase-dead mutant protein failed to accumulate in PODs and also prevented Daxx translocation to PODs in response to apoptotic stimuli, IFN-γ, and arsenic oxide. Furthermore, we also identified proapoptotic protein prostate apoptosis response 4 (Par-4) as a substrate of ZIPK and found that Par-4 facilitates the association between ZIPK and Daxx. Small-interfering RNA (siRNA)-mediated reductions in the expression of endogenous ZIPK, Daxx, or Par-4 revealed that the complex is necessary for activation of caspases and induction of apoptosis triggered by IFN-γ and arsenic oxide. Thus, ZIPK represents a new component of PODs, which mediates apoptosis from nuclei.

MATERIALS AND METHODS

Antibodies. Two kinds of polyclonal antisera recognizing ZIPK were generated in rabbits by using synthetic peptides as immunogens. Peptides were synthesized with an N-terminal cysteine appended to permit conjugation to maleimide-activated carrier protein keyhole limpet hemocyanin (Sawady Technology Co. Ltd., Tokyo, Japan). The peptides used as immunogens were CRDGSAGLG RDLRRLRTELG, corresponding to residues 362 to 381 of murine ZIPK (Ab1), and GLRELQRGRRQCRERVCALR, representing amino acids (aa) 338 to 352 of murine ZIPK (Ab2). New Zealand White rabbits were injected with a mixture of peptide and Freund's complete adjuvant and then boosted three times at monthly intervals with peptide in Freund's incomplete adjuvant, before blood was collected and immune serum was obtained (Sawady Technology Co. Ltd.).

Anti-Daxx (M-112, H-7), anti-Par-4 (R-334, A-10), anti-PML (PG-M3, H-238), and anti-Myc (9E10) antibodies were purchased from Santa Cruz Biotechnology, Inc. Anti-FLAG (M2) and anti-hemagglutinin (HA) (3F10) monoclonal antibodies were purchased from Sigma and Roche, respectively.

Plasmids. The plasmids encoding epitope-tagged ZIPK, ZIPK K42A, ZIPK ΔLZ, DAPK2 K52A, Daxx, and Daxx ΔC and Tpl2 were described previously (23, 24, 48). The cDNAs encoding mouse Par-4 (full-length), Par-4 LZ (aa 232 to 323), and Par-4 ΔLZ (aa 1 to 278) were amplified by PCR using a mouse placenta cDNA library (Clontech). Expression plasmid pEF-BOS was digested with *Xba*I to remove the stuffer sequence, blunted with T4 polymerase, and ligated with a *Sal*I linker. Fragments of Par-4 which were epitope tagged at their N termini were generated by PCR, digested with *Sal*I, and inserted into this modified pEF-BOS plasmid. The sequences of DNA fragments obtained by PCR were confirmed by DNA sequencing. The cDNAs encoding full-length Par-4, Par-4 LZ, and Par-4 ΔLZ were then amplified by PCR from these plasmids and subcloned in frame into the yeast two-hybrid plasmid pACT-2 for expressing chimeric proteins with a Gal4 *trans*-activation domain.

Two-hybrid screening. Yeast two-hybrid screening was performed using the Matchmaker two-hybrid system (Clontech) as described previously (23). To construct a bait plasmid, the LZ domain of murine ZIPK (aa 398 to 448) was cloned in-frame with the DNA-binding domain of GAL4 in the plasmid pAS2-1. *Saccharomyces cerevisiae* Y190 cells were transformed with the ZIPK bait plasmid by a modified lithium acetate method, and the transformants were selected on synthetic dextrose medium lacking tryptophan (SD Trp). The transformants grown on SD Trp were sequentially transformed with a mouse brain cDNA library fused to the GAL4 *trans*-activation domain in pACT2 (Clontech). A total of 2×10^7 transformants were screened on plates lacking tryptophan, leucine, and histidine and containing 25 mM 3-aminotriazole. The resulting colonies were then assayed for β-galactosidase activity by filter assays where color was scored after 1 h of incubation at 37°C. Positive clones were picked, the pACT2 library plasmids were recovered from individual β-galactosidase-positive clones and expanded in *Escherichia coli*, and the cDNA inserts were sequenced.

Cell culture and transfection. Human embryonic kidney HEK293 and HEK293T cells, human cervix carcinoma HeLa cells, and monkey COS-7 cells were grown in high-glucose Dulbecco's modified Eagle's medium containing 4.5 g of glucose/dl supplemented with 10% fetal calf serum, 1 nM L-glutamine, and antibiotics. For transient transfections, cells were transfected with various plasmids by using SuperFect reagent (Qiagen) according to the manufacturer's instructions. Experiments were performed after 1 to 3 days.

Indirect immunofluorescence microscopy. HeLa cells (10^3) cultured on eight-well Lab-Tek chamber slides (Nalge Nunc International) were transiently transfected with a total of 50 ng of plasmid DNA by using a combination of Lipofectamine and Lipofectamine Plus reagents (Invitrogen). After 24 h, cells were treated with 1,500 U of IFN-γ/ml or 1.0 μM As_2O_3. The cells were fixed with 4% paraformaldehyde in phosphate-buffered saline (pH 7.4) containing 0.1% Tween 20 (PBS-T) for 15 min at room temperature. After fixation, cells were washed with PBS-T and permeabilized for 5 min with 0.1% saponin (Sigma) in PBS-T. The cells were blocked with PBS-T containing 2.5% goat serum (Sigma), 1.0% bovine serum albumin (Sigma), and 0.1% saponin (30 min, 20°C) and then incubated for 1 h at room temperature with the primary antibody diluted in blocking solution (1:200 for anti-Daxx, 1:500 for anti-FLAG or anti-Myc). Following this incubation, cells were rinsed five times for 2 min in blocking solution at room temperature and then incubated with 8 μg of fluorescein isothiocyanate (FITC)-conjugated anti-mouse or rhodamine-conjugated anti-rabbit immunoglobulin G (IgG; Dako)/ml for 1 h at room temperature. Excess secondary antibody was washed off 10 times for 2 min with blocking buffer. For double staining, after the secondary FITC-conjugated anti-mouse antibody was washed off, cells were incubated with a rabbit polyclonal antibody (1:1,000) for 1 h at room temperature. After five washes, cells were incubated with 8 μg of rhodamine-conjugated anti-rabbit IgG/ml for 1 h. After 10 washes, the slides were covered with Vectashield mounting medium containing 1.5 μg of 4′,6-diamidino-2′-phenylindole dihydrochloride (DAPI; Vector Laboratories)/ml and glass coverslips were applied. Cells were imaged with a Bio-Rad MRC 1024 instrument.

Coimmunoprecipitation and immunoblotting. HEK293, HEK293T, and COS-7 cells ($\sim 10^6$) were transiently transfected with a total of 4 μg of expression plasmids. After 24 to 48 h, cells were suspended in lysis buffer containing 20 mM Tris (pH 7.5), 0.5% NP-40, 150 mM NaCl, 0.2 mM phenylmethylsulfonyl fluoride (PMSF), and 10 μg of aprotinin/ml and passed through a 21-gauge needle 20 times to break nuclei. Debris was removed by centrifugation, and the cleared supernatants were incubated with a combination of 30 μl of recombinant protein G-Sepharose beads (Zymed) and 1.0 μg of antibody at 4°C for 12 h. For detection of endogenous protein interactions, lysates were prepared from 3×10^8 cells. Immunoprecipitates were washed with 1.5 ml of lysis buffer four times and suspended in Laemmli sample buffer. Immune complexes were separated by sodium dodecyl sulfate-polyacrylamide gel electrophoresis (SDS-PAGE), followed by transfer to nitrocellulose filters. Blots were incubated with various primary antibodies. After incubation with horseradish peroxidase-conjugated secondary antibodies against mouse IgG or rabbit IgG (Amersham Pharmacia), the blots were developed by the enhanced chemiluminescence detection method (Dupont) with exposure to X rays (Kodak).

In vitro kinase assay. COS-7 cells (10^6) transiently transfected with 4.0 μg of expression plasmids were lysed with NP-40 lysis buffer (0.5% NP-40, 150 mM NaCl, 10 mM Tris-HCl [pH 7.5], 1 mM EDTA, 0.2 mM PMSF, 10 μg of aprotinin/ml). Following preclearing, the lysates were immunoprecipitated with a combination of 1.0 μg of antibody and 30 μl of protein G-Sepharose beads. The immunoprecipitates were washed four times with lysis buffer and once with kinase reaction buffer (10 mM $MgCl_2$, 3 mM $MnCl_2$, 10 mM Tris-HCl [pH 7.2]). In vitro kinase reactions were performed for 10 min at 30°C in 20 μl of kinase reaction buffer containing 10 μCi of [γ-^{32}P]ATP. Laemmli sample buffer was added to terminate the reactions. After boiling for 5 min, the samples were separated by SDS-PAGE. Phosphorylated proteins were visualized by autoradiography.

Cell death assays. HEK293 and HeLa cells were transfected with various plasmids in combination with pEGFP (Clontech). After 36 to 48 h of culture, the

percentage of apoptotic cells that showed membrane blebbing was determined by fluorescence microscopy, counting 300 green fluorescent protein (GFP)-positive cells. Alternatively, both floating and attached cells were collected, fixed, and incubated in 1.0 μg of DAPI/ml. The percentage of cells with fragmented nuclei or condensed chromatin was determined by fluorescence microscopy, counting a minimum of 300 cells. As_2O_3 and recombinant human IFN-γ were purchased from Sigma and R&D, respectively.

Caspase assays. Cytosolic extracts from HeLa and HEK293 cells were prepared in buffer A (10 mM KCl, 1.5 mM $MgCl_2$, 1 mM EDTA, 1 mM EGTA, 1 mM dithiothreitol, 0.1 mM PMSF, 20 mM HEPES-KOH [pH 7.4]) as described previously (10). After protein concentrations were measured with the DC protein assay kit (Bio-Rad), 30-μg protein samples were incubated with fluorogenic caspase substrate acetyl-Asp-Glu-Val-Asp-aminofluorocoumarin (Ac-DEVD-AFC; Calbiochem) in 100 μl of caspase buffer consisting of 1 mM EDTA, 0.1% CHAPS {3-[(3-cholamidopropyl)-dimethylammonio]-1-propanesulfonate}, 10% sucrose, and 25 mM HEPES-KOH (pH 7.2). Caspase activity was measured by using an LS550B fluorometric plate reader (Perkin-Elmer) in the kinetic mode with excitation and emission wavelengths of 405 and 510 nm, respectively. Releases of AFC from the substrate peptide were compared after a 30-min incubation.

Transfection of siRNAs. For siRNA experiments, double-stranded RNA duplexes composed of annealed 21-nucleotide sense and antisense oligoribonucleotides were synthesized by Dharmacon Research (Lafayette, Colo.). RNA oligonucleotides used for targeting ZIPK, Daxx, and Par-4 in this study were as follows: ZIPK-S, 5′-CAUCCUGCGGGAGAUCCGGdTdT-3′; ZIPK-AS, 5′-CCGGAUCUCCCGCAGGAUGdTdT-3′; Daxx-S, 5′-CCUCUAUAACCGGCAGCAAdTdT-3′; Daxx-AS, 5′-UUGCUGCCGGUUAUAGAGGdTdT-3′; Par-4-S, 5′-GAUGCAAUUACACAACAGAdTdT-3′; Par-4-AS, 5′-UCUGUUGUGUAAUUGCAUCdTdT-3′. Ten microliters of 20 μM double-stranded RNAs was preincubated with 15 μl of Oligofectamine reagent (Invitrogen) in 400 μl of serum-free Opti-MEM medium for 20 min before use. HeLa cells were plated on 60-mm-diameter dishes at 2×10^5 cells 12 h before transfection, washed with serum-free Opti-MEM, and then incubated with an siRNA-Oligofectamine mixture at 37°C for 4 h, followed by addition of 3 ml of fresh medium containing 10% fetal calf serum. At 36 to 48 h after transfection, cells were stimulated with IFN-γ or As_2O_3 for various times and then analyzed for apoptosis or lysed for immunoblotting or caspase assay.

RESULTS

ZIPK translocates to PODs in response to As_2O_3 and IFN-γ. To understand the mode of action of ZIPK in apoptosis, we sought to analyze the subcellular localization of this kinase using immunofluorescence. HeLa cells were transiently transfected with an expression plasmid encoding FLAG-tagged ZIPK and then stained with an anti-FLAG antibody. ZIPK localized to nuclei, displaying a diffuse nuclear pattern in ~70% of transfected cells, while in ~30% of cells, ZIPK localized to nuclei with a speckled pattern, consisting typically of 10 to 20 dot-like structures per nucleus (Fig. 1A).

Treatment of APL cells with arsenicals such as As_2O_3 is known to restore PML-RARα oncoproteins to PODs, and, in normal cells, As_2O_3 recruits PML to PODs (55). In addition, IFNs are known to up-regulate PML at the transcriptional level, leading to a significant increase in the size and number of PODs (28, 40, 46). We therefore analyzed the localization of ZIPK before and after stimulation with IFN-γ and As_2O_3. Approximately 80% of cells expressing FLAG-ZIPK displayed the nuclear speckled pattern after stimulation with As_2O_3 or IFN-γ (Fig. 1A and B), compared to only ~30% of unstimulated cells.

To confirm that the nuclear structures to which ZIPK localizes are PODs, endogenous PML was simultaneously stained with an anti-PML polyclonal antibody in HeLa cells (Fig. 1C). Prior to stimulation, PML was present in nuclei with either a predominantly diffuse pattern or a speckled pattern with a few dots, depending on the cell examined. In contrast, the number of dots (PODs) increased in response to As_2O_3 and IFN-γ. Moreover, under these conditions, FLAG-ZIPK colocalized with endogenous PML (Fig. 1C). Quantification of the percentage of specks showing colocalization of PML and ZIPK revealed a change from 24% before treatment ($n = 100$) to 82 and 89% after treatment with As_2O_3 and IFN, respectively ($n = 100$ PODs counted).

Cellular localization of endogenous Daxx was also investigated with an anti-Daxx antibody, since we and others previously showed that Daxx colocalizes with PML in PODs in various cell lines (29, 48, 53). As shown in Fig. 1D, Daxx was present in nuclei with a diffuse pattern in nonstimulated HeLa cells but translocated to PODs in response to As_2O_3 and IFN-γ. Under these conditions, FLAG-ZIPK also colocalized with endogenous Daxx (Fig. 1D). Contrary to previous reports that Daxx associates with Fas or transforming growth factor β receptors in the cytoplasm (36, 51), we did not observe cytoplasmic localization of Daxx in cells (Fig. 1D).

ZIPK associates with Daxx. Colocalization of ZIPK with Daxx prompted us to ask whether these molecules physically associate. Cell lysates prepared from HEK293T cells transiently transfected with a plasmid encoding FLAG-Daxx were immunoprecipitated with control rabbit IgG or two different anti-ZIPK antibodies by using equal volumes of the same lysate. The resulting immune complexes were then tested for the presence of associated Daxx by immunoblotting. As shown in Fig. 2A, FLAG-Daxx was coimmunoprecipitated with either of two anti-ZIPK antibodies employed for immunoprecipitations but not when the control antibody was used, indicating association of endogenous ZIPK with overexpressed Daxx in HEK293T cells. Similar results were obtained by coexpressing FLAG-tagged ZIPK with HA-Daxx in HEK293T cells and using an anti-FLAG antibody (instead of anti-ZIPK) to prepare immunoprecipitates (Fig. 2B). Moreover, full-length Daxx, as well as a truncation mutant Daxx lacking the C-terminal region (Daxx ΔC), was coimmunoprecipitated with ZIPK, indicating that the N-terminal domain of Daxx (residues 1 to 625) is sufficient for binding. In contrast, neither full-length Daxx nor Daxx ΔC was coimmunoprecipitated with the anti-FLAG antibody in cells that had been transfected with FLAG-Tpl2, a protein kinase belonging to the MAP3K family, thus confirming the specificity of the results (Fig. 2B).

Interaction of endogenous ZIPK and endogenous Daxx was also examined by coimmunoprecipitation experiments using HeLa cells and antibodies specific for either ZIPK (rabbit antiserum) or Daxx (mouse monoclonal antibody). Prior to stimulation with IFN-γ or As_2O_3, little or no ZIPK coimmunoprecipitated with Daxx (Fig. 2C). In contrast, after 12 h stimulation with IFN-γ or As_2O_3, interaction between Daxx and ZIPK was detectable by coimmunoprecipitation assay. Immunoblot analysis of lysates prepared from the same cells demonstrated that IFN-γ and As_2O_3 did not change the levels of ZIPK or Daxx in HeLa cells (Fig. 2C). We conclude, therefore, that ZIPK inducibly binds to Daxx in response to IFN-γ and As_2O_3.

A mutant ZIPK prevents Daxx translocation to PODs in response to IFN-γ and As_2O_3. Apoptosis induction by ZIPK depends on its catalytic activity (23). This suggests that kinase-inactive mutant versions of ZIPK might act as dominant-neg-

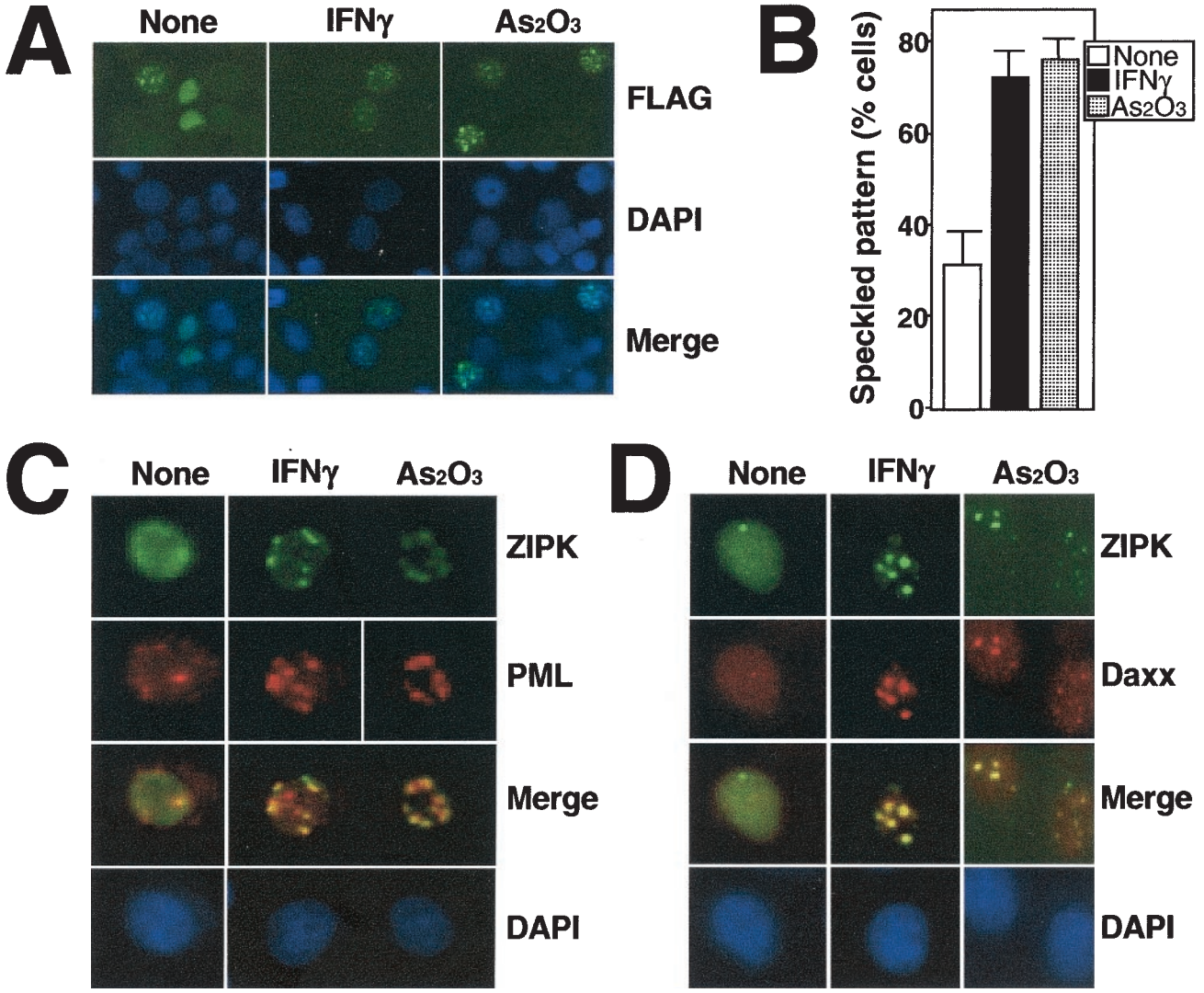

FIG. 1. ZIPK colocalizes with Daxx in PODs. (A) HeLa cells grown on coverslips were transiently transfected with FLAG-ZIPK. After 36 h of transfection, cells were stimulated with 1,500 U of IFN-γ/ml or 1.0 μM As_2O_3 for 12 h. After fixation, cells were stained with an anti-FLAG antibody (M2) for the detection of ZIPK and DAPI for visualization of nuclei. Antibody detection was achieved with a FITC-conjugated anti-mouse antibody (green), followed by microscopy analysis. The bottom panels show the overlay result. (B) HeLa cells transiently transfected with FLAG-ZIPK were stimulated with IFN-γ and As_2O_3 for 12 h and stained with an anti-FLAG antibody, and the percentage of transfected cells with a speckled pattern was determined by counting a minimum of 200 transfected cells. Data represent means ± standard deviations ($n = 3$). (C and D) HeLa cells transiently transfected with FLAG-ZIPK were stimulated with IFN-γ or As_2O_3 for 12 h and stained sequentially with an anti-FLAG monoclonal antibody (top), an anti-PML polyclonal antibody (C, upper middle), or an anti-Daxx polyclonal antibody (D, upper middle) and DAPI (bottom). Antibody detection was achieved with a FITC-conjugated anti-mouse antibody (green) and a rhodamine-conjugated anti-rabbit antibody (red). Overlay results (merge) demonstrate colocalization of FLAG-ZIPK and PML or Daxx in response to IFN-γ and As_2O_3.

ative inhibitors of the endogenous ZIPK, particularly since ZIPK dimerizes via its LZ domain (23). To explore this possibility, we generated ZIPK K42A, a mutant protein in which lysine 42 in the ATP-binding site was converted to alanine, destroying catalytic activity. To explore the effect of this kinase-inactive mutant protein on Daxx localization to PODs, HeLa cells were transiently transfected with FLAG-ZIPK K42A and then stimulated with As_2O_3 or IFN-γ for 6 and 18 h, respectively, after which cells were doubly stained with anti-FLAG monoclonal and anti-Daxx polyclonal antibodies and imaged by confocal microscopy. Unlike the wild-type ZIPK, ZIPK K42A was present in nuclei in a diffuse pattern, failing to target to PODs even after stimulation with IFN-γ or As_2O_3 (Fig. 3A). Notably, IFN-γ- and As_2O_3-inducible translocation of Daxx to PODs was dramatically inhibited in cells expressing ZIPK K42A, suggesting that ZIPK mediates Daxx translocation to PODs through its catalytic activity (Fig. 3B). ZIPK K42A was also expressed into HeLa cells and tested for its effect on translocation of PML to PODs. Unlike Daxx, ZIPK K42A did not interfere with PML localization to nuclear

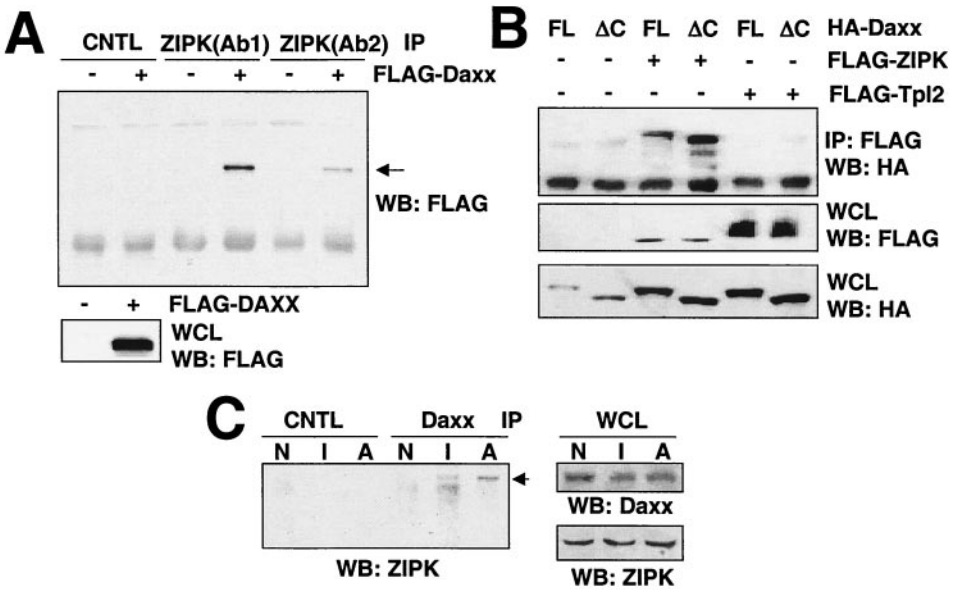

FIG. 2. ZIPK associates with Daxx. (A) One million 293T cells were transiently transfected with 2.0 μg of plasmid DNA encoding FLAG-tagged Daxx. After 36 h, cell lysates were immunoprecipitated (IP) with control rabbit anti-mouse Ig serum, anti-ZIPK (Ab1), or another anti-ZIPK antibody (Ab2). Proteins were separated by SDS-PAGE, transferred to nitrocellulose, and blotted with an anti-FLAG monoclonal antibody (top). Aliquots of whole-cell lysates (WCL) were simultaneously subjected to immunoblot analysis using an anti-FLAG antibody (bottom). WB, Western blotting. (B) 293T cells were transiently transfected with the indicated combinations of HA-Daxx (FL), HA-Daxx ΔC (ΔC), FLAG-ZIPK, and FLAG-Tpl2. Total amounts of plasmids were kept constant at 6.0 μg by supplementation with the empty pcDNA3 plasmid. After 36 h, cell lysates were immunoprecipitated with an anti-HA monoclonal antibody, followed by Western blotting with an anti-FLAG antibody (top). Aliquots of whole-cell lysates were simultaneously subjected to immunoblot analysis using an anti-FLAG (middle) or anti-HA antibody (bottom). (C) HeLa cells (3×10^8) were stimulated with IFN-γ or As_2O_3 for 12 h. Cell lysates were prepared, and immunoprecipitated with a monoclonal Daxx or control (CNTL) antibody. The immunoprecipitates were separated by SDS-PAGE, followed by blotting with an anti-ZIPK antibody (Ab1). Aliquots of the whole-cell lysates were simultaneously subjected to Western blot analysis using an anti-Daxx or anti-ZIPK antibody as indicated. N, nonstimulated; I, IFN-γ; A, As_2O_3.

speckles in response to IFN-γ and As_2O_3, demonstrating that translocation of Daxx to PODs was specifically prevented by expression of ZIPK K42A (Fig. 3C and D).

Identification of Par-4 as a ZIPK-interacting protein. To further identify ZIPK-interacting proteins, we carried out a yeast two-hybrid screen of a mouse brain cDNA library using the LZ domain of ZIPK as a bait. From a screen of $\sim 2 \times 10^7$ transformants, 32 positive clones were identified. Sequence analysis revealed that 9 of these clones encoded portions of the Par-4 protein, while 12 clones encoded ATF4 and 7 clones encoded ZIPK (consistent with the ability of this protein to self-associate) (23).

Par-4 was originally identified as a molecule induced in prostate cancer cells undergoing apoptosis induced by androgen withdrawal (44). Par-4 carries an LZ domain at its C terminus and a death domain-like structure at its N terminus (12). Several reports have suggested that Par-4 is involved in apoptosis, sensitizing cells to certain apoptosis stimuli (1, 18, 33).

The interaction of ZIPK with Par-4 was initially confirmed by coimmunoprecipitation experiments using epitope-tagged proteins expressed by transient transfection in HEK293T cells (not shown), followed by a demonstration that endogenous ZIPK interacts with endogenous Par-4, as determined by coimmunoprecipitation experiments using specific antibodies (Fig. 4A). For the immunoprecipitation experiments shown in Fig. 4A, the same cell lysate was divided into equal-volume aliquots to ensure loading equivalent amounts of protein.

Next, the region responsible for the interaction of ZIPK and Par-4 was determined by yeast two-hybrid assays. As shown in Fig. 4B, the C-terminal LZ domain of ZIPK was necessary and sufficient for interaction with the C-terminal LZ of Par-4. Thus, ZIPK and Par-4 associate via their LZ domains, contrary to a prior report (34). To confirm the dependence on the LZ for association of ZIPK and Par-4 in mammalian cells, coimmunoprecipitation experiments were performed using COS-7 cells transiently transfected with a plasmid encoding FLAG-tagged ZIPK together with plasmids encoding Myc-tagged Par-4, Myc-tagged Par-4 ΔLZ, or Myc-tagged Par-4 LZ. As shown in Fig. 4C, FLAG-ZIPK coimmunoprecipitated with the anti-Myc antibody in cells transfected with Myc–Par-4 and Myc–Par-4 LZ but not with Myc–Par-4 ΔLZ. Thus, the LZ of Par-4 is required for its association with ZIPK in mammalian cells.

The ability of ZIPK to bind Par-4 prompted us to test if Par-4 is a substrate of this kinase. To this end, COS-7 cells were transiently transfected with plasmids encoding Myc–Par-4 along with FLAG-tagged wild-type ZIPK or ZIPK K42A. Cells were then lysed, and immunoprecipitations were performed with the anti-Myc antibody, followed by in vitro kinase assays using [γ-^{32}P]ATP. Consistent with a prior report (34), phosphorylated Myc–Par-4 was seen in immunoprecipitates from cells expressing FLAG-tagged wild-type ZIPK, suggesting that Par-4 is phosphorylated by ZIPK (Fig. 4D). In contrast, when Par-4 was coimmunoprecipitated with kinase-

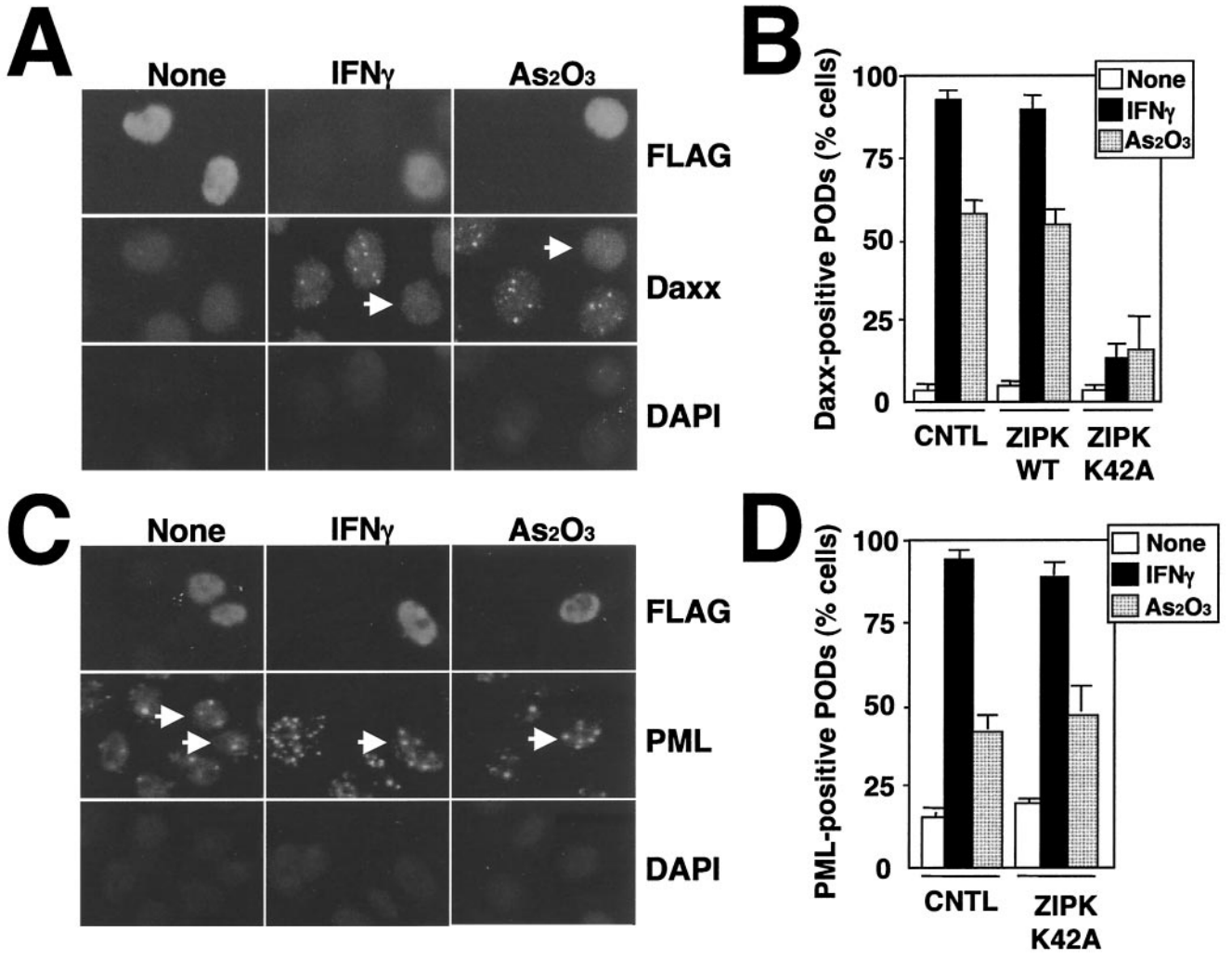

FIG. 3. ZIPK K42A prevents Daxx translocation into PODs in response to IFN-γ and As_2O_3. (A) HeLa cells were transiently transfected with FLAG-ZIPK K42A. After 36 h of transfection, cells were stimulated with As_2O_3 or IFN-γ for 6 or 18 h, respectively. The cells were fixed and stained sequentially with an anti-FLAG antibody (top), an anti-Daxx antibody (middle), and DAPI (bottom). Arrows, cells expressing FLAG-ZIPK K42A. Note that Daxx translocation to PODs was prevented by expression of ZIPK K42A. (B) Cells were prepared as for panel A. The percentage of transfected cells with Daxx translocation to PODs is presented, counting at least 200 transfected cells from three independent experiments (means ± standard deviations [SD]). CNTL, control; WT, wild type. (C) HeLa cells were transiently transfected with FLAG-ZIPK K42A. After 36 h of transfection, cells were stimulated with As_2O_3 or IFN-γ for 6 or 18 h, respectively. The cells were fixed and stained sequentially with an anti-FLAG antibody (top), an anti-PML antibody (middle), and DAPI (bottom). Arrows, cells expressing FLAG-ZIPK K42A. Note that PML translocation to PODs was not affected by expression of ZIPK K42A. (D) Cells were prepared as for panel C. Shown are the percentages of cells with PML translocation to PODs, counting at least 200 transfected cells from three independent experiments (means ± SD).

dead ZIPK K42A, phosphorylation was not observed, indicating that phosphorylation of Par-4 depends on the catalytic activity of ZIPK (Fig. 4D). Neither autophosphorylation of ZIPK nor phosphorylation of Par-4 changed in response to IFN-γ and As_2O_3 (not shown).

Next, Myc–Par-4 was introduced into HeLA cells and the cellular localization was determined by staining with the anti-Myc antibody. As shown in Fig. 4E, Myc–Par-4 was observed in both the nucleus and cytoplasm, but not in PODs. Furthermore, Myc–Par-4 did not move to PODs in response to IFN-γ and As_2O_3 (data not shown). We presume, therefore, that Daxx disassociates from Par-4 after exposure of cells to IFN-γ and As_2O_3.

Collaborative interactions of Par-4, ZIPK, and Daxx. Since ZIPK can associate with Daxx and Par-4, we wished to determine whether these interactions are mutually exclusive or mutually supportive. First, we tested whether Par-4 can bind Daxx by coimmunoprecipitation assays using HEK293T cells overexpressing Myc–Par-4 with either FLAG-Daxx or FLAG-ZIPK. As shown in Fig. 5A, Myc–Par-4 was coimmunoprecipitated with FLAG-ZIPK but not FLAG-Daxx, suggesting that Par-4 does not directly bind Daxx. Analysis of the cell lysates demonstrated equivalent amounts of Myc–Par-4 production, excluding differences in the levels of this protein as a trivial explanation for the differential binding of Daxx and ZIPK.

To further explore the structure-function requirements for

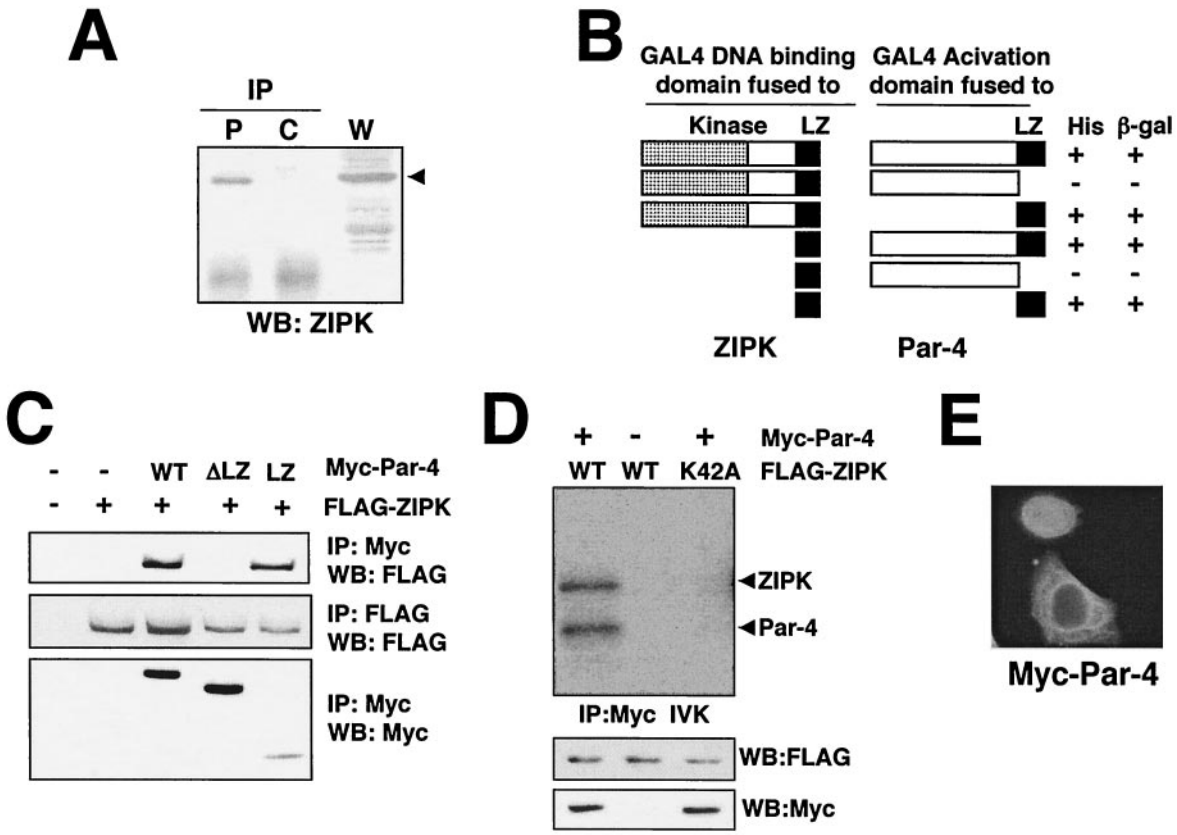

FIG. 4. ZIPK binds and phosphorylates Par-4. (A) Cell lysates prepared from HeLa cells (3×10^8) were divided into equal volumes and used for immunoprecipitation (IP) with an anti-Par-4 monoclonal antibody (P) or control IgG (C), followed by immunoblotting with an anti-ZIPK antibody (Ab1). Aliquots of whole-cell lysates (W) were simultaneously subjected to immunoblot analysis using an anti-ZIPK antibody. WB, Western blotting. Arrowhead, band corresponding to ZIPK. (B) Plasmids expressing ZIPK or mutant versions of it fused to the GAL4 DNA-binding domain were cotransformed with a plasmid expressing Par-4 or various mutant proteins fused to the GAL4 *trans*-activation domain. Interactions were detected on the basis of the ability of cells to grow on medium lacking leucine, tryptophan, and histidine (+). β-Gal, β-galactosidase. (C) COS-7 cells were transiently transfected with the indicated combinations of plasmids encoding FLAG-ZIPK, Myc–wild-type Par-4 (WT), Myc–Par-4 ΔLZ (ΔLZ), or Myc–Par-4 LZ (LZ), holding the amounts of DNA at 5.0 μg by addition of an empty vector. Cell lysates were immunoprecipitated with an anti-Myc antibody (9E10), followed by immunoblot analysis using an anti-FLAG antibody (M2) as indicated. (D) COS-7 cells were transiently transfected with the indicated combinations of plasmids. After 36 h, cell lysates were immunoprecipitated with an anti-Myc antibody and subjected to in vitro kinase assays. Aliquots of whole-cell lysates were simultaneously subjected to immunoblot analysis using an anti-FLAG or anti-Myc antibody. IVK, in vitro kinase assay. (E) HeLa cells grown on coverslips were transiently transfected with Myc–Par-4. At 36 h after transfection, cells were stained with an anti-Myc monoclonal antibody. Antibody detection was achieved by using a FITC-conjugated anti-mouse antibody.

ZIPK-mediated enhancement of Par-4 association with Daxx, we compared wild-type ZIPK with ZIPK K42A and ZIPK ΔLZ. For these experiments, HEK293T cells were transfected with Myc–Par-4 and FLAG-Daxx, alone or in combination with plasmids encoding HA-ZIPK, HA-ZIPK K42A, or HA-ZIPK ΔLZ (Fig. 5B). In the absence of coexpressed ZIPK, FLAG-Daxx was not coimmunoprecipitated with Myc–Par-4 (lane 3). In the presence of wild-type HA-ZIPK, however, FLAG-Daxx was coimmunoprecipitated with Myc–Par-4 (lane 4). In contrast, coexpressing HA-ZIPK (K42A) (lane 5) or HA-ZIPK ΔLZ (lane 6) did not result in association of Daxx and Par-4 (Fig. 5B). These results suggest that ZIPK-induced association of Par-4 and Daxx requires both the LZ domain of ZIPK and catalytic activity of this kinase.

Finally, we next examined the effect of Par-4 on the association of ZIPK and Daxx. For these experiments, HEK293T cells were transiently transfected with FLAG-Daxx, with or without Myc–Par-4 and lysates were immunoprecipitated with an anti-ZIPK antibody, followed by analysis of the resulting immune complexes by immunoblotting using an anti-FLAG antibody to detect Daxx-associated ZIPK. As shown in Fig. 5C, the association of endogenous ZIPK with FLAG-Daxx was enhanced by coexpression of Par-4. Similar results were obtained when the epitope tag on Daxx was switched to HA and immunoprecipitations were performed with FLAG-ZIPK instead of endogenous ZIPK (Fig. 5D). These findings suggest that Par-4, Daxx, and ZIPK may form a ternary complex, though further work is required to verify this hypothesis.

ZIPK, Daxx, and Par-4 collaborate in caspase activation and apoptosis induction. Previous reports indicated that overexpressing ZIPK, Par-4, or Daxx induces apoptosis (23, 33, 48). Since ZIPK, Par-4, and Daxx appear to form a protein complex, we explored the effects of combined expression of these proteins on apoptosis induction. For these experiments, plas-

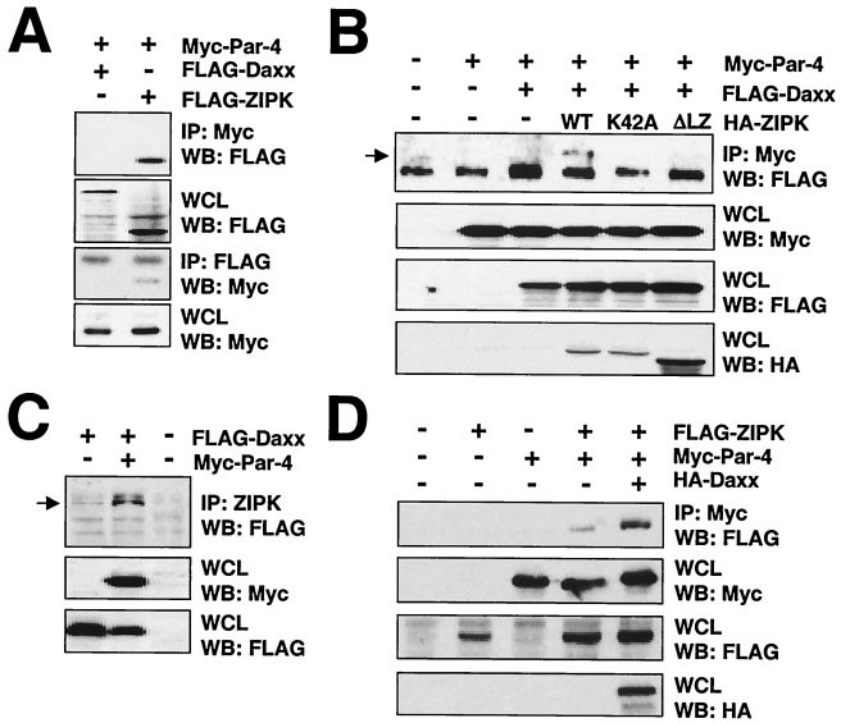

FIG. 5. Par-4 facilitates the association between ZIPK and Daxx. (A) 293T cells (10^6 cells) were transiently transfected with 2.0 μg of Myc–Par-4 together with 2.0 μg of FLAG-Daxx or FLAG-ZIPK. Cell lysates were immunoprecipitated (IP) with an anti-Myc or anti-FLAG antibody, followed by immunoblot analysis using an anti-FLAG or anti-Myc antibody, as indicated. WB, Western blotting; WCL, whole-cell lysates. (B) 293T cells (10^6 cells) were transiently transfected with the indicated combinations of plasmids encoding Myc–Par-4, FLAG-Daxx, HA–wild-type (WT) ZIPK, HA-ZIPK K42A, or HA-ZIPK ΔLZ. Total amounts of DNA were kept at 6.0 μg. Cell lysates were immunoprecipitated with an anti-Myc antibody, followed by immunoblot analysis using an anti-FLAG antibody (top). Aliquots of whole-cell lysates were simultaneously subjected to immunoblot analysis using an anti-Myc (upper middle), anti-FLAG (lower middle), or anti-HA (bottom) antibody. (C) 293T cells (10^6 cells) were transiently transfected with 2.5 μg of expression plasmids encoding Myc–Par-4 and FLAG-Daxx as indicated. Total amounts of DNA were held at 5.0 μg by addition of an empty vector. After 36 h, cells were lysed and immunoprecipitated with an anti-ZIPK antibody (Ab1), followed by immunoblot analysis using an anti-FLAG antibody. Aliquots of the whole-cell lysates were simultaneously subjected to immunoblot analysis using an anti-FLAG or anti-Myc antibody. (D) 293T cells (10^6 cells) were transiently transfected with the indicated combinations of plasmids encoding FLAG-ZIPK, Myc–Par-4, and HA-Daxx, holding total amounts of DNA at 6.0 μg by addition of an empty vector. Cell lysates were immunoprecipitated with an anti-Myc antibody, followed by immunoblot analysis using an anti-FLAG antibody. Aliquots of whole-cell lysates were simultaneously subjected to immunoblot analysis using an anti-Myc, anti-FLAG, or anti-HA antibody.

mids encoding these proteins were expressed along with a GFP marker plasmid in HEK293 cells, identifying the apoptotic GFP-positive cells. Cells transfected individually with plasmids encoding ZIPK, Par-4, or Daxx did not exhibit an increase in apoptosis at the concentrations of plasmid DNA used here (Fig. 6A). In contrast, the percentage of apoptotic cells was increased two- to threefold in cultures of cells coexpressing ZIPK with either Par-4 or Daxx (Fig. 6A). Similarly, coexpressing Daxx with Par-4 elevated the percentage of apoptotic cells by two to threefold compared to the percentage due to expression of either Daxx or Par-4 alone (Fig. 6A). The most striking increase in apoptosis, however, was achieved by expressing all three proteins together. When expressed together, ZIPK, Daxx, and Par-4 induced an approximately sixfold increase in apoptosis.

The activation of caspases represents a sine qua non for apoptosis (6, 39, 47). We therefore tested the effects of overexpressing ZIPK, Par-4, and Daxx individually and in combination on activation of caspases in HEK293 cells. Caspase activity in cytosolic cell extracts was measured based on hydrolysis of fluorogenic substrate Ac-DEVD-AFC. As shown in Fig. 6B, expression individually of ZIPK, Daxx, or Par-4 failed to induce significant increases in caspase activity in HEK293 cells. In contrast, expression in combination of ZIPK, Daxx, and Par-4 induced substantial elevations in caspase activity, approximately threefold above baseline. Thus, ZIPK, Daxx, and Par-4 collaborate in activating caspases when overexpressed.

Next, the effect of expression of mutant ZIPK, Par-4, and Daxx (ZIPK K42A, Par-4 LZ, and Daxx ΔC, respectively) on apoptosis induction was examined. As shown in Fig. 6C, the percentage of apoptotic cells was increased approximately sixfold in cultures of cells coexpressing wild-type ZIPK, Par-4, and Daxx compared to the percentage in control cultures. In contrast, increased apoptosis was not observed in cells overexpressing ZIPK K42A along with Par-4 and Daxx. Likewise, apoptosis was not induced in cells expressing Par-4 LZ along with ZIPK and Daxx or in cells expressing Daxx ΔC along with ZIPK and Par-4. These results suggest that collaborative effects among ZIPK, Par-4, and Daxx are necessary for induction of apoptosis.

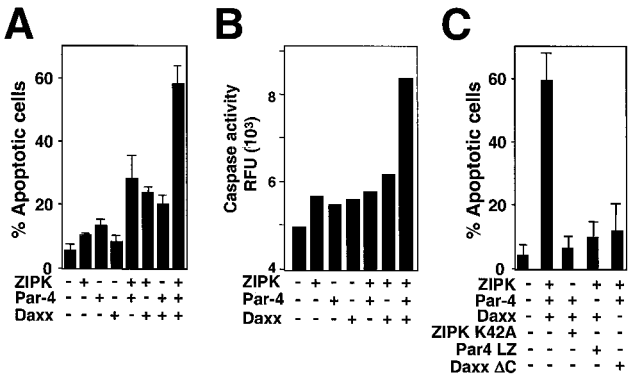

FIG. 6. Induction of cell death by ZIPK, Daxx, and Par-4. (A) 293T cells (5×10^5 cells) were transiently cotransfected with the indicated combinations of plasmids (total, 3.0 μg) together with 0.3 μg of a GFP expression plasmid. After 48 h, GFP-positive cells were evaluated by microscopy, and the percentages of GFP-positive cells with apoptotic morphology were determined, counting 200 cells (means ± standard deviations [SD]; $n = 3$). (B) 293T cells were transiently cotransfected with the indicated combinations of plasmids (total, 3.0 μg). After 48 h, cytoplasmic proteins were extracted and caspase activity was measured, with Ac-DEVD-AFC as the substrate. Data represent relative fluorescence units (RFU) normalized for protein concentration (means ± SD; $n = 3$). (C) 293T cells (5×10^5 cells) were transiently cotransfected with the indicated combinations of plasmids (total, 3.0 μg) together with 0.3 μg of GFP expression plasmids. After 48 h, the percentages of GFP-positive apoptotic cells were determined, counting 200 cells (means ± SD; $n = 3$).

IFN-γ and As_2O_3 induce PML expression and apoptosis. Since IFN-γ and As_2O_3 enhance POD formation and facilitate recruitment of ZIPK and Daxx into PODs, we wished to explore the effects of these agents on expression of POD-targeted genes and apoptosis. First, we compared the levels of ZIPK, Daxx, Par-4, and PML proteins in HeLa cells before and after stimulation with As_2O_3 or IFN-γ by immunoblot analysis. As shown in Fig. 7A, stimulation with As_2O_3 or IFN-γ induced increases in PML protein levels without affecting expression of the ZIPK, Daxx, or Par-4 proteins. IFN-γ induced sustained increases in PML, while As_2O_3 only transiently induced PML (Fig. 7A). These increases in PML protein levels were accompanied by increases in the number and size of PODs to which Daxx was colocalized (Fig. 7B).

Since increases in PODs have been correlated with induction of apoptosis, we next examined the effects of As_2O_3 and IFN-γ on apoptosis in cultures of HeLa cells. Both As_2O_3 and IFN-γ triggered cell death, with <20% of cells remaining viable at 4 days posttreatment (Fig. 7C). As_2O_3 and IFN-γ also induced caspase activation in HeLa cells, as measured by Ac-DEVD-AFC hydrolysis (Fig. 7D). Thus, these agents stimulate POD formation and induce caspase activation and cell death.

Dominant-negative mutant ZIPK and Par-4 suppress apoptosis induced by POD-stimulating agents. As suggested in Fig. 6, either ZIPK K42A or Par-4 LZ might function as a dominant-negative mutant protein to prevent apoptosis. Indeed, previous reports indicated that the LZ domain of Par-4 can function as a dominant-negative inhibitor of apoptosis (18). Therefore, we introduced ZIPK K42A and Par-4 LZ into HeLa cells to inhibit endogenous activity of ZIPK and Par-4. HeLa cells transfected with either ZIPK K42A or Par-4 LZ were treated with As_2O_3 or IFN-γ for 3 days, followed by determination of the number of apoptotic cells by DAPI staining. As a control for specificity, we also transfected cells with a dominant-negative version of the related kinase DAPK2, which similarly contained a mutated ATP-binding site (K52A). As shown in Fig. 8, the percentage of cells undergoing apoptosis in response to As_2O_3 or IFN-γ was decreased when either ZIPK K42A or Par-4 LZ, but not DAPK2 K52A, was expressed. In contrast, the percentage of transfected cells undergoing apoptosis was not changed when cells were stimulated with staurosporine (STS) instead of As_2O_3 or IFN-γ, showing the specificity of the effect of dominant-negative ZIPK K42A and Par-4 LZ proteins on apoptosis induced by agents that affect PODs.

siRNA-mediated suppression of ZIPK, Daxx, and Par-4 reveals a requirement for IFN-γ- and As_2O_3-induced apoptosis. To explore whether ZIPK, Daxx, and Par-4 are necessary for induction of apoptosis and activation of caspases by As_2O_3 and IFN-γ, we used siRNA to reduce endogenous expression of these genes in HeLa cells. In pilot experiments, the sequences of double-stranded 21-mer RNAs were optimized, until active siRNA reagents were obtained. For each siRNA, double-stranded RNA controls with mismatches relative to the target mRNA were prepared. The specific siRNA for ZIPK, Par-4, or Daxx or negative-control RNAs was transfected into HeLa cells, and cell lysates were prepared 2 days later for immunoblot analysis, which confirmed reduced expression of each of the targeted genes but no effect on the expression of other genes (Fig. 9A). Furthermore, reduced expression of these genes was maintained up to 6 days, as determined by immunoblot analysis (data not shown).

Next, we determined the effects of these siRNAs on HeLa cell death induced by IFN-γ and As_2O_3 (Fig. 9B). Knocking down expression of ZIPK, Daxx, and Par-4 individually resulted in significant reductions of cell death 3 days after exposure to IFN-γ and As_2O_3. In contrast, apoptosis induced by STS was not affected (not shown).

We also measured caspase activity in HeLa cells treated with siRNA and either IFN-γ or As_2O_3. Caspase activity induced after the stimulation with IFN-γ and As_2O_3 was strikingly reduced by 60 to 80% in HeLa cells treated with siRNA targeting either ZIPK, Par-4, or Daxx (Fig. 9C). In contrast, caspase activity induced by STS was not inhibited by treatment with siRNA targeting ZIPK, Daxx, or Par-4 (not shown).

DISCUSSION

The ZIPK/DAPK family comprises five members: ZIPK (Dlk), DAPK, DRAK1, DRAK2, and DAPK2 (DRP1) (4, 26, 45). Although overexpression of active ZIPK was previously shown to induce apoptosis, the mechanism of how this kinase is regulated in cells and the identity of its specific substrates of relevance to apoptosis are unclear. In this study, we demonstrated that ZIPK is a nuclear protein which is present in PODs, initiating an apoptotic pathway from within nuclei in collaboration with proapoptotic proteins Daxx and Par-4.

PODs have been implicated in a wide variety of cellular processes, including transcriptional regulation, tumor suppression, growth suppression, cellular senescence, and apoptosis (42). To date, more than 30 proteins reportedly localize to

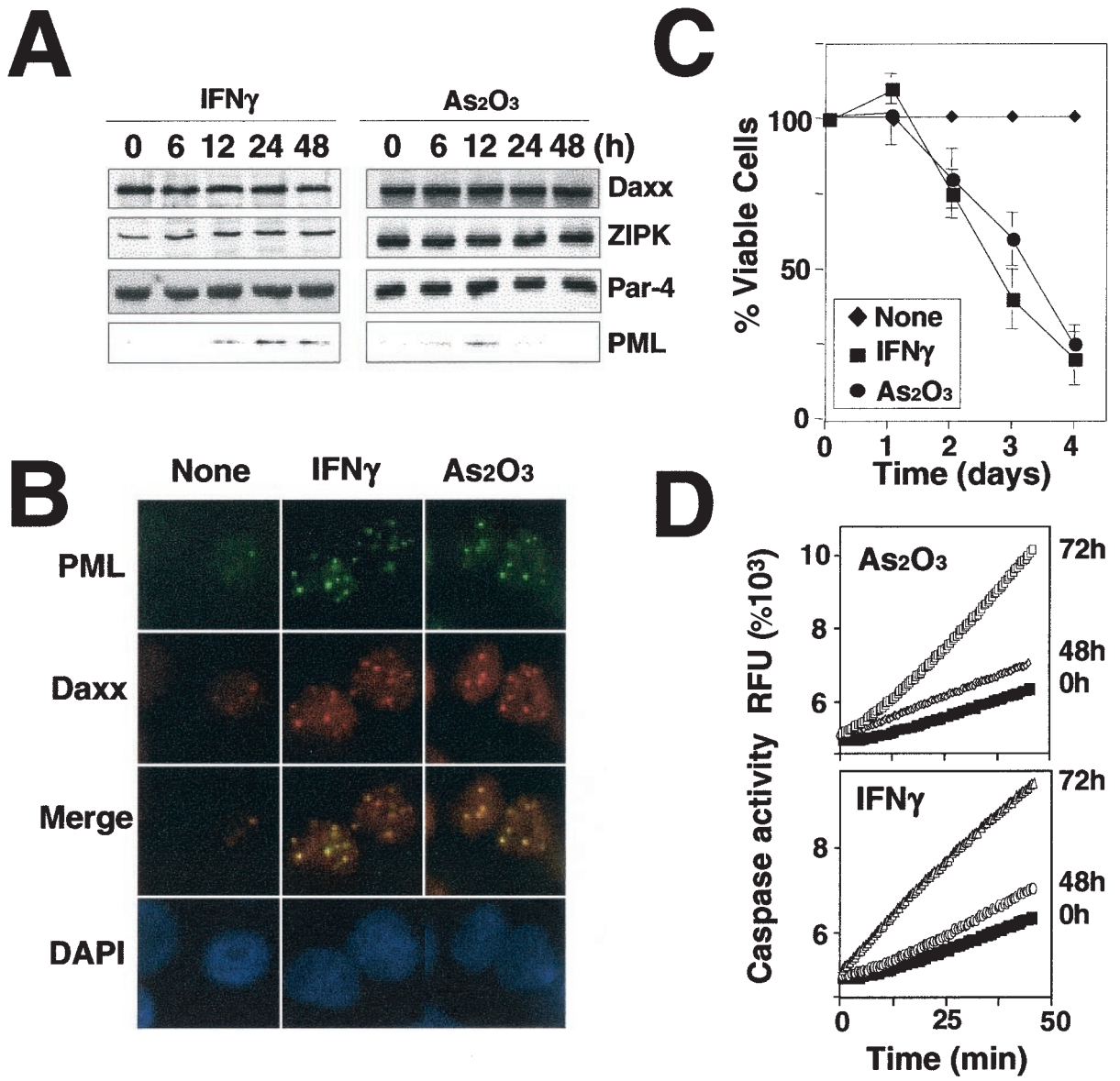

FIG. 7. As_2O_3 and IFN-γ induce POD formation and apoptosis. (A) Immunoblot analysis of ZIPK, Par-4, and Daxx in HeLa cells was performed using cell lysates normalized for total protein content (50 μg per lane) and specific antibodies that detect the endogenous proteins. Cells were stimulated for the indicated times with 1,500 U of IFN-γ/ml or 1.0 μM As_2O_3 prior to lysis. (B) HeLa cells stimulated for 12 h with IFN-γ or As_2O_3 were fixed and stained with an anti-PML monoclonal antibody and a FITC-conjugated anti-mouse IgG secondary antibody (top) and then stained with an anti-Daxx polyclonal antibody and a rhodamine-conjugated anti-rabbit secondary antibody (upper middle) and DAPI (bottom). Overlay results (merge) demonstrate colocalization of PML and Daxx in response to IFN-γ and As_2O_3. Cells were imaged by fluorescence microscopy. (C) HeLa cells were treated with IFN-γ and As_2O_3 for the indicated periods. The percentage (Å) of viable cells was determined by DAPI staining, counting a minimum of 300 cells (means ± standard errors; $n = 3$). (D) HeLa cells were stimulated with As_2O_3 or IFN-γ for 48 or 72 h. Cytoplasmic proteins were extracted, and the caspase activity was measured, with Ac-DEVD-AFC as the substrate. RFU, relative fluorescence units.

these nuclear structures (42). Among the POD-associated proteins, evidence supporting roles for PML and Daxx in apoptosis regulation has been provided by studies of PML-deficient mice and of antisense-mediated reduction in Daxx expression, as well as PML and Daxx overexpression experiments (14, 37, 48, 50, 53). However, little is known about the biochemical mechanism by which these proteins modulate apoptosis-relevant pathways. In this regard, while it was originally reported that Daxx binds the death domain of Fas and signals apoptosis by direct interactions with the MAP3K protein Ask-1 (3), these results have been difficult to substantiate, and in most types of cells Daxx is found exclusively in the nucleus and therefore unable to associate with Fas or Ask-1 (3, 51). Furthermore, in contrast to wild-type Daxx, a mutant Daxx that failed to localize to PODs was unable to enhance Fas-induced apoptosis (48), suggesting that Daxx participates in apoptosis regulation

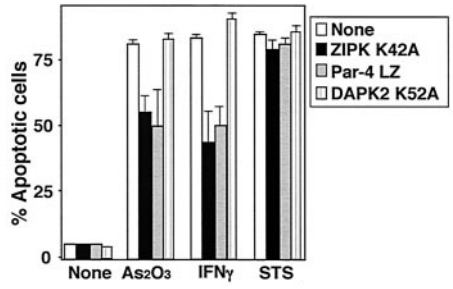

FIG. 8. Dominant-negative ZIPK and Par-4 suppress apoptosis induced by POD-stimulating agents. 293T (5×10^5) cells were transiently cotransfected with the indicated plasmids (total, 3.0 μg), together with 0.3 μg of the GFP expression plasmid. After 12 h, cells were stimulated with 1,500 U of IFN-γ/ml, 1.0 μM As_2O_3, or 100 μM STS. After 3 days (IFN-γ and As_2O_3) or 24 h (STS) of incubation, the percentages of GFP-positive apoptotic cells were determined, counting 200 cells (means ± standard deviations; $n = 3$).

through its association with PODs. Notably, the localization of Daxx into PODs is disrupted in PML-deficient cells, whereas introduction of exogenous PML into PML-deficient cells causes relocalization of Daxx to PODs (53). Moreover, forced expression of Daxx induces apoptosis in $PML^{+/+}$ cells but not in $PML^{-/-}$ cells, indicating that Daxx localization within PODs is required for apoptosis induction (53).

Our finding that endogenous ZIPK inducibly associates with endogenous Daxx in response to IFN-γ and As_2O_3, and that it controls Daxx targeting into PODs via its catalytic activity suggests an important role for this apoptosis-inducing protein kinase in control of the POD-mediated pathway for apoptosis. Consistent with this idea, the kinase-negative mutant protein ZIPK (K42A) specifically prevented translocation of Daxx, but not PML, into PODs and suppressed apoptosis induced by As_2O_3 and IFN-γ, but not by other types of stimuli. Thus, ZIPK may sensitize cells to apoptosis by recruiting Daxx to PODs through its kinase activity.

It remains to be defined what signals control activation of ZIPK. In this regard, we did not observe an increase in the activity of ZIPK in response to As_2O_3 and IFN-γ (data not shown). Instead, we found that the location of ZIPK changed from diffusely nuclear to discretely POD associated in response to those stimuli. Thus, the proapoptotic activity of ZIPK might be regulated by its cellular localization. Perhaps Daxx brings ZIPK into close proximity with upstream activators of this kinase within PODs. Alternatively, Daxx could carry ZIPK to the PODs, helping to bring it into contact with apoptosis-relevant substrates in these nuclear structures. In this regard, it is believed that all inputs to apoptosis pathways ultimately converge on caspases, resulting in their activation. Certain caspases can be found in the nucleus, raising the possibility of an interaction of ZIPK with these proteases (35). However, it has also been reported that overexpressing ZIPK without its LZ domain results in cytosolic accumulation of this kinase and induces apoptosis, implying an apoptosis-relevant target of this kinase in the cytosol (25, 34). In our experiments, however, ZIPK ΔLZ remained within nuclei and was not found in the

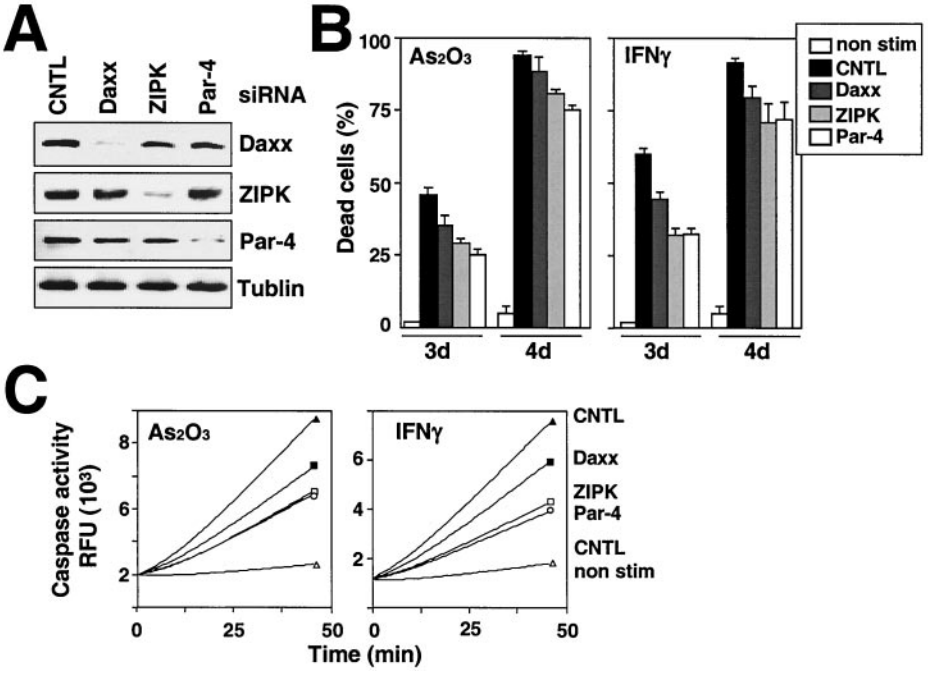

FIG. 9. ZIPK, Daxx, and Par-4 are necessary for apoptosis mediated by As_2O_3 and IFN-γ, as determined by using siRNA. (A) HeLa cells were transfected with siRNA targeting ZIPK, Daxx, or Par-4, and cells were analyzed by immunoblotting using anti-ZIPK, anti-Daxx, anti-Par-4, and anti-tubulin antibodies, verifying siRNA-mediated reduction in endogenous ZIPK, Daxx, and Par-4. CNTL, control. (B) HeLa cells were treated with siRNA. After 24 h, cells were stimulated with IFN-γ or As_2O_3 for 3 or 4 days. The percentages of apoptotic cells were determined by DAPI staining, counting a minimum of 300 cells (means ± standard errors; $n = 3$). (C) HeLa cells were treated with siRNA. After 24 h, cells were stimulated with IFN-γ or As_2O_3 for 4 days. Extracts prepared from HeLa cells or after treatment with siRNA were tested for the activation of caspase 3, based on the release of AFC from the Ac-DEVD-AFC substrate.

cytosol, suggesting that the LZ is not necessary for nuclear sequestration of ZIPK and that the substrates of ZIPK relevant to apoptosis reside in the nucleus (23). However, ZIPK has been reported to phosphorylate the myosin II regulatory light chain (32), at least when overexpressed. Thus further work is needed to resolve the issue of where the apoptosis-relevant substrates of ZIPK reside.

The kinase activity of ZIPK ΔLZ was strikingly decreased compared to that of the wild-type protein. Furthermore, induction of apoptosis by ZIPK ΔLZ was also decreased compared to that by the wild-type protein. Thus, the LZ appears to be necessary for the full activation of ZIPK, as well as for induction of apoptosis, although the LZ is not necessary for localization of ZIPK within PODs. Since Par-4 does not appear to enter PODs, however, we presume that the role of Par-4 occurs prior to IFN-γ- or As_3O_2-induced translocation of Daxx and ZIPK to PODs. Thus, we favor the idea that Par-4 is an activator in the POD-dependent apoptosis pathway rather than an effector.

Using an unbiased yeast two-hybrid interaction cloning method, we discovered that ZIPK associates with Par-4. ZIPK also appears to induce phosphorylation of Par-4, at least in vitro. Par-4 was originally identified as a molecule induced in prostate cancer cells undergoing apoptosis induced by androgen withdrawal (44). Subsequently, it was shown that Par-4 can promote apoptosis. The mechanisms proposed for Par-4-mediated apoptosis are quite varied, including direct or indirect effects on transcription of apoptosis-regulatory genes and suppression of atypical protein kinase Cs (PKCs) (11, 12, 41). Par-4 carries an LZ domain at its C terminus and a death domain-like structure at its N terminus (12). The interaction of ZIPK and Par-4 is mediated by their LZs. Overexpression of Par-4 enhanced association between ZIPK and Daxx. Likewise, overexpression of ZIPK, but not ZIPK K42A, induced association of Par-4 and Daxx, suggesting that, once phosphorylated by ZIPK, Par-4 might act as scaffold to facilitate interactions between ZIPK and Daxx. Par-4 also collaborated with ZIPK and Daxx in inducing apoptosis when all three proteins were overexpressed in cells. Conversely, siRNA-mediated knockdown of Par-4 resulted in suppression of apoptosis induced by IFN-γ and As_2O_3. Importantly, in experiments where the LZ of Par-4 was overexpressed, apoptosis induced by IFN-γ and As_2O_3 was suppressed, implying a role for Par-4 or the proteins with which its LZ binds in the POD-mediated pathway for apoptosis. Thus, we propose that Par-4 represents an additional component of the POD-mediated pathway for apoptosis. The biochemical mechanism by which Par-4 contributes to this unique pathway for apoptosis remains to be determined. Conceivably, the interaction of the LZ of Par-4 with the LZ of ZIPK could serve as a mechanism for activating ZIPK or stabilizing its interactions with substrates or with adapter proteins that recruit this kinase into PODs. However, a report that Par-4 binds PKCζ, suppressing its activity, also raises the possibility that Par-4 could inhibit ZIPK activity, though this seems unlikely given the requirement for intact kinase activity for ZIPK-mediated apoptosis (12).

Since the LZ domain of ZIPK binds to the LZs of both ATF4 and Par-4, competition is expected to occur (23). In normal conditions, ZIPK is held by nuclear transcription factor ATF4 in the nucleus, whereas, in response to POD-inducing stimuli, ZIPK moves to PODs in association with Daxx and binds and phosphorylates Par-4. Par-4 might compete with ATF4 for binding to ZIPK, thus releasing ZIPK from ATF4 to trigger apoptosis. Consistent with this idea, it has been reported that coexpression of ATF4 with ZIPK suppresses apoptosis (23). These observations suggest that ZIPK is latent or inactive when binding to ATF4 in the nucleus and that its apoptotic potential is unmasked when it enters into the PODs, in association with Daxx. Previously, others have also identified Par-4 as a ZIPK-interacting protein (34). In coexpression studies, they showed that Par-4 enhanced ZIPK-induced apoptosis, purportedly by encouraging ZIPK to exit the nucleus and accumulate in the cytosol. However, in HeLa cells, we found that Par-4 is present in both cytosol and nuclei, and its location did not change after stimulation with IFN-γ and As_2O_3. Further work is required to clarify the mechanism by which Par-4 collaborates with ZIPK and Daxx in initiating apoptosis from PODs.

ACKNOWLEDGMENTS

We thank P. N. Tsichlis for Tpl2 plasmid, S.-I. Matsuzawa and H. Marusawa for helpful discussions, F. Nomura for technical assistance, and J. Valois and R. Cornell for manuscript preparation.

T.K. was supported by postdoctoral fellowships from the Japan Society for the Promotion of Science, and the University of California, Tobacco-Related Disease Research Program (10FT-0311). This work was also supported by NIH grant CA69381.

REFERENCES

1. **Camandola, S., and M. P. Mattson.** 2000. Pro-apoptotic action of PAR-4 involves inhibition of NF-κB activity and suppression of BCL-2 expression. J. Neurosci. Res. **61:**134–139.
2. **Cardone, M. H., N. Roy, H. R. Stennicke, G. S. Salvesen, T. F. Franke, E. Stanbridge, S. Frisch, and J. C. Reed.** 1998. Regulation of cell death protease caspase-9 by phosphorylation. Science **282:**1318–1320.
3. **Chang, H., H. Nishitoh, X. Yang, H. Ichijo, and D. Baltimore.** 1998. Activation of apoptosis signal-regulating kinase 1 (ASK1) by the adapter protein daxx. Science **281:**1860–1863.
4. **Cohen, O., and A. Kimchi** 2001. DAP-kinase: from functional gene cloning to establishment of its role in apoptosis and cancer. Cell Death Differ. **8:**6–15.
5. **Cohen, O., E. Feinstein, and A. Kimchi.** 1997. DAP-kinase is a Ca^{2+}/calmodulin-dependent, cytoskeletal-associated protein kinase, with cell death-inducing functions that depend on its catalytic activity. EMBO J. **16:**998–1008.
6. **Cryns, V., and J. Yuan.** 1999. Proteases to die for Genes Dev. **12:**1551–1570.
7. **Datta, S. R., H. Dudek, X. Tao, S. Masters, H. Fu, Y. Gotoh, and M. E. Greenberg.** 1997. Akt phosphorylation of BAD couples survival signals to the cell-intrinsic death machinery. Cell **91:**231–241.
8. **Deiss, L. P., E. Feinstein, H. Berissi, O. Cohen, and A. Kimchi.** 1995. Identification of a novel serine/threonine kinase and a novel 15-kD protein as potential mediators of the gamma interferon-induced cell death. Genes Dev. **9:**15–30.
9. **de The, H., C. Lavau, A. Marchio, C. Chomienne, L. Degos, and A. Dejean.** 1991. The PML-RAR alpha fusion mRNA generated by the t(15;17) translocation in acute promyelocytic leukemia encodes a functionally altered RAR. Cell **66:**675–684.
10. **Deveraux, Q. L., R. Takahashi, G. S. Salvesen, and J. C. Reed.** 1997. X-linked IAP is a direct inhibitor of cell death proteases. Nature **388:**300–304.
11. **Diaz-Meco, M. T., M. J. Lallena, A. Monjas, S. Frutos, and J. Moscat.** 1999. Inactivation of the inhibitory κB protein kinase/nuclear factor κB pathway by Par-4 expression potentiates tumor necrosis factor alpha-induced apoptosis. J. Biol. Chem. **274:**19606–19612.
12. **Diaz-Meco, M. T., M. M. Municio, S. Frutos, P. Sanchez, J. Lozano, L. Sanz, and J. Moscat.** 1996. The product of par-4, a gene induced during apoptosis, interacts selectively with the atypical isoforms of protein kinase C. Cell **86:**777–786.
13. **Ferri, K. F., and G. Kroemer.** 2001. Organelle-specific initiation of cell death pathways. Nat. Cell Biol. **3:**255–263.
14. **Gongora, R., R. P. Stephan, Z. Zhang, and M. D. Cooper.** 2001. An essential role for Daxx in the inhibition of B lymphopoiesis by type I interferons. Immunity **14:**723–737.
15. **Green, D., and G. Evan.** 2002. A matter of life and death. Cancer Cell **1:**19–30.

16. **Green, D. R., and J. C. Reed.** 1998. Mitochondria and apoptosis. Science **281:**1309–1312.
17. **Guo, A., P. Salomoni, J. Luo, A. Shih, S. Zhong, W. Gu, and P. P. Pandolfi.** 2000. The function of PML in p53-depedent apoptosis. Nat. Cell Biol. **2:**730–736.
18. **Guo, Q., W. Fu, J. Xie, H. Luo, S. Sells, J. W. Geddes, V. Bonada, V. Rangnekar, and M. Mattson.** 1998. Par-4 is a mediator of neuronal degeneration associated with the pathogenesis of Alzheimer's disease. Nat. Med. **4:**957–962.
19. **Ichijo, H., E. Nishida, K. Irie, P. P. ten Dijke, M. Saitoh, T. Moriguchi, M. Takagi, K. Matsumoto, K. Miyazono, and Y. Y. Gotoh.** 1997. Induction of apoptosis by ASK1, a mammalian MAPKKK that activates SAPK/JNK and p38 signaling pathways. Science **275:**90–94.
20. **Inbal, B., O. Cohen, S. Polak-Charcon, J. Kopolovic, E. Vadai, L. Eisenbach, and A. Kimchi.** 1997. DAP kinase links the control of apoptosis to metastasis. Nature **390:**180–184.
21. **Inbal, B., G. Shani, O. Cohen, J. L. Kissil, and A. Kimchi.** 2000. Death-associated protein kinase-related protein 1, a novel serine/threonine kinase involved in apoptosis. Mol. Cell. Biol. **20:**1044–1054.
22. **Kakizuka, A., W. Miller, K. Umesono, R. Warrell, S. Frankel, V. Murty, E. Dmitrovsky, and R. Evans.** 1991. Chromosomal translocation t(15;17) in human acute promyelocytic leukemia fuses RAR alpha with a novel putative transcription factor, PML. Cell **66:**663–674.
23. **Kawai, T., M. Matsumoto, K. Takeda, H. Sanjo, and S. Akira.** 1998. ZIP kinase, a novel serine/threonine kinase which mediates apoptosis. Mol. Cell. Biol. **18:**1642–1651.
24. **Kawai, T., F. Nomura, K. Hoshino, N. G. Copeland, D. J. Gilbert, N. A. Jenkins, and S. Akira.** 1999. Death-associated protein kinase 2 is a new calcium/calmodulin-dependent protein kinase that signals apoptosis through its catalytic activity. Oncogene **18:**3471–3480.
25. **Kogel, D., O. Plottner, G. Landsberg, S. Christian, and K. H. Scheidtmann.** 1998. Cloning and characterization of Dlk, a novel serine/threonine kinase that is tightly associated with chromatin and phosphorylates core histones. Oncogene **17:**2645–2654.
26. **Kogel, D., J. H. Prehn, and K. H. Scheidtmann.** 2001. The DAP kinase family of pro-apoptotic proteins: novel players in the apoptotic game. Bioessays **23:**352–358.
27. **Kojima, H., A. Nemoto, T. Uemura, R. Honma, M. Ogura, and Y. Liu.** 2001. rDrak1, a novel kinase related to apoptosis, is strongly expressed in active osteoclasts and induces apoptosis. J. Biol. Chem. **276:**19238–19243.
28. **Lavau, C., A. Marchio, M. Fagioli, J. Jansen, B. Falini, P. Lebon, F. Grosveld, P. P. Pandolfi, P. G. Pelicci, and A. Dejean.** 1995. The acute promyelocytic leukemia-associated PML gene is induced by interferon. Oncogene **11:**871–876.
29. **Li, H., C. Leo, J. Zhu, X. Wu, J. O'Neil, E.-J. Park, and J. D. Chen.** 2000. Sequestration and inhibition of Daxx-mediated transcriptional repression by PML. Mol. Cell. Biol. **20:**1784–1796.
30. **Locksley, R. M., N. Killeen, and M. J. Lenardo.** 2001. The TNF and TNF receptor superfamilies: integrating mammalian biology. Cell **104:**487–501.
31. **Motyka, B., G. Korbutt, M. J. Pinkoski, J. A. Heibein, A. Caputo, M. Hobman, M. Barry, I. Shostak, T. Sawchuk, C. F. Holmes, J. Gauldie, and R. C. Bleackley.** 2000. Mannose 6-phosphate/insulin-like growth factor II receptor is a death receptor for granzyme B during cytotoxic T cell-induced apoptosis. Cell **103:**491–500.
32. **Murata-Hori, M., Y. Fukuta, K. Ueda, T. Iwasaki, and H. Hosoya.** 2001. HeLa ZIP kinase induces diphosphorylation of myosin II regulatory light chain and reorganization of actin filaments in nonmuscle cells. Oncogene **20:**8175–8183.
33. **Nalca, A., S. G. Qiu, N. El-Guendy, S. Krishnan, and V. M. Rangnekar.** 1999. Oncogenic Ras sensitizes cells to apoptosis by Par-4. J. Biol. Chem. **274:**29976–29983.
34. **Page, G., D. Kogel, V. Rangnekar, and K. H. Scheidtmann.** 1999. Interaction partners of Dlk/ZIP kinase: co-expression of Dlk/ZIP kinase and Par-4 results in cytoplasmic retention and apoptosis. Oncogene **18:**7265–7273.
35. **Paroni, G., C. Henderson, C. Schneider, and C. Brancolini.** 2002. Caspase-2 can trigger cytochrome c release and apoptosis from the nucleus. J. Biol. Chem. **277:**15147–15161.
36. **Perlman, R., W. P. Schiemann, M. W. Brooks, H. F. Lodish, and R. A. Weinberg.** 2001. TGF-beta-induced apoptosis is mediated by the adapter protein Daxx that facilitates JNK activation. Nat. Cell Biol. **3:**708–714.
37. **Quignon, F., F. De Bels, M. Koken, J. Feunteun, J.-C. Ameisen, and H. de Thé.** 1998. Pml induces a novel caspase-independent death process. Nat. Genet. **20:**259–265.
38. **Raveh, T., G. Droguett, M. S. Horwitz, R. A. DePinho, and A. Kimchi.** 2000. DAP-kinase activates a p19ARF/p53-mediated apoptotic checkpoint to suppress oncogenic transformation. Nat. Cell Biol. **3:**1–7.
39. **Reed, J. C.** 2002. Apoptosis-based therapies. Nat. Rev. Drug Discov. **1:**111–121.
40. **Regad, T., and M. K. Chelbi-Alix.** 2001. Role and fate of PML nuclear bodies in response to interferon and viral infections. Oncogene **20:**7274–7286.
41. **Richard, D. J., V. Schumacher, B. Royer-Pokora, and S. G. Roberts.** 2001. Par4 is a coactivator for a splice isoform-specific transcriptional activation domain in WT1. Genes Dev. **15:**328–339.
42. **Salomoni, P., and P. P. Pandolfi.** 2002. The role of PML in tumor suppression. Cell **108:**165–170.
43. **Sanjo, H., T. Kawai, and S. Akira.** 1998. DRAKs, novel serine/threonine kinases related to death-associated protein kinase that trigger apoptosis. J. Biol. Chem. **273:**29066–29071.
44. **Sells, S. F., D. P. Wood, S. S. Joshi-Barve, Jr., S. Muthukumar, R. J. Jacob, S. A. Crist, S. Humphreys, and V. M. Rangnekar.** 1994. Commonality of the gene programs induced by effectors of apoptosis in androgen-dependent and -independent prostate cells. Cell Growth Differ. **5:**457–466.
45. **Shohat, G., G. Shani, M. Eisenstein, and A. Kimchi.** 2002. The DAP-kinase family of proteins: study of a novel group of calcium-regulated death-promoting kinases. Biochim. Biophys. Acta **1600:**45–50.
46. **Stadler, M., M. K. Chelbi-Alix, M. H. Koken, L. Venturini, C. Lee, A. Saib, F. Quignon, L. Pelicano, M. C. Guillemin, C. Schindler, et al.** 1995. Transcriptional induction of the PML growth suppressor gene by interferon is mediated through an ISRE and GAS element. Oncogene **11:**2565–2573.
47. **Thornberry, N. A., and Y. Lazebnik.** 1998. Caspases: enemies within. Science **281:**1312–1316.
48. **Torii, S., D. A. Egan, R. A. Evans, and J. C. Reed.** 1999. Human daxx regulates fas-induced apoptosis from nuclear pml oncogenic domains (pods). EMBO J. **18:**6037–6049.
49. **Wallach, D., E. E. Varfolomeev, N. L. Malinin, Y. V. Goltsev, A. V. Kovalenko, and M. P. Boldin.** 1999. Tumor necrosis factor receptor and Fas signaling mechanisms. Annu. Rev. Immunol. **17:**331–367.
50. **Wang, Z.-G., D. Ruggero, S. Ronchetti, S. Zhong, M. Gaboli, R. Rivi, and P. P. Pandolfi.** 1998. Pml is essential for multiple apoptotic pathways. Nat. Genet. **20:**266–272.
51. **Yang, X., R. Khosravi-Far, H. Y. Chang, and D. Baltimore.** 1997. Daxx, a novel Fas-binding protein that activates JNK and apoptosis. Cell **89:**1067–1076.
52. **Zha, J., H. Harada, E. Yang, J. Jockel, and S. J. Korsmeyer.** 1996. Serine phosphorylation of death agonist BAD in response to survival factor results in binding to 14–3–3 not BCL-XL Cell **87:**619–628.
53. **Zhong, S., P. Salomoni, S. Ronchetti, A. Guo, D. Ruggero, and P. P. Pandolfi.** 2000. Promyelocytic leukemia protein (PML) and daxx participate in a novel nuclear pathway for apoptosis. J. Exp. Med. **191:**631–639.
54. **Zhou, B. P., Y. Liao, W. Xia, Y. Zou, B. Spohn, and M. C. Hung.** 2001. HER-2/neu induces p53 ubiquitination via Akt-mediated MDM2 phosphorylation. Nat. Cell Biol. **3:**973–982.
55. **Zhu, J., M. Koken, Q. Frederique, M. Chelbi-Alix, L. Degos, Z. Wang, Z. Chen, and H. de The.** 1997. Arsenic-induced PML targeting onto nuclear bodies: implications for the treatment of acute promyelocytic leukemia Proc. Natl. Acad. Sci. USA **94:**3978–3983.